Agronomy Research **19**(S1), 777–787, 2021
https://doi.org/10.15159/AR.21.027

Thermo mechanical vibration of single wall carbon nanotube partially embedded into soil medium

M. Hossain* and J. Lellep

University of Tartu, Faculty of Science and Technology, Institute of mathematics and statistics, Narva mnt 18, EE51009 Tartu, Estonia
*Correspondence: mainul.hossain@ut.ee

Received: January 2nd, 2021; Accepted: April 2nd, 2021; Published: April 7th, 2021

Abstract. Single wall carbon nanotube is one of the promising forms of carbon nanocomposite. Due to its high strength and stiffness, carbon nanotube is potentially used in various nanoscale structures. In this paper, dynamic behaviour of single wall carbon nanotube partially embedded into elastic soil medium is modelled by the Euler-Bernoulli beam theory and nonlocal theory of elasticity. Analytical solution technique is employed to solve these governing differential equations of nanotube. Analysing the effects of temperature, nonlocal parameter, coefficients of elastic medium on dynamic behaviour of nanotube are our main concern. The results reveal that the effects of temperature, nonlocal parameter and coefficients of elastic medium are very significant on the natural frequency of nanotube.

Key words: carbon nanotube, partially embedded, elastic soil medium, temperature effect, exact solution technique.

INTRODUCTION

Carbon nanotube is very promising and effective element that has been used for developing high-performance composites. The main advantages of the carbon nanotube are its high chemical stability as well as its strong mechanical properties. In this paper, thermal effects on the dynamic behaviour of nanotube embedded into the soil (Haldar & Basu, 2013; Zhao et al., 2016; Zhang et al., 2018; Elhuni & Basu, 2019; Falope et al., 2020) or elastic medium are investigated. Soil can be considered as an elastic foundation. Basically, Winkler's model is used to simulate the soil foundation. According to Winkler's model, foundation is demonstrated by a series of discrete infinitesimal and mutually independent, closely spaced, linearly elastic lateral springs which provide resistance in direct proportion to its deflection. This model is very simple and popular among researchers. However, this model is unable to include the soil cohesive force or shear force. That is why Winkler's model is not sufficient for evaluating the mechanical behaviour of soil. To overcome the limitation of Winkler's model, Pasternak proposed two parameters model which included the transverse shear deformation. The advantages of this model are considering compressive stiffness and shear resistance which simulate the soil as a continuum. Moreover, surrounding temperature effects (Askari &

Esmailzadeh, 2017; Jiang & Wang, 2017; Lai & Zhang, 2018; Aria et al., 2019) on nanotube are also very important. Sometimes, researchers ignore the thermal effects. Whereas, the thermal effects on dynamic behaviour of nanostructure are very significant for designing nanostructure effectively. Dynamic characteristic of structure is significantly affected by the thermal load induced from temperature variation. Specially, lightweight structure such as nanotube is crucially affected by temperature where this element is extensively used in different nanocomposites. The end restrictions of the structural element are very important to induce the thermal effect. If the structure is restrained on the boundaries, it can't elongate freely that induces thermal stress inside the restrained structure. This thermal stress is very critical for nanomaterial and can be the cause of failure. Nevertheless, the temperature can change material properties. For instance, Young's modulus, density of nanotube can be significantly reduced by the rise of temperature.

Researchers extensively investigated the single wall carbon nanotube due to its high demand in material and technology. The nanotube is modelled based on various theories such as Timoshenko beam theory (Jiang et al., 2017), Shear deformation theory (Malikan et al., 2018), and Euler beam theory (Ehteshami & Hajabasi, 2011). Dynamic behaviour of nanotube is also very popular topic among researchers. Chang (2017) investigated nonlinear vibration of single-walled carbon nanotubes under the longitudinal magnetic field. He concluded that the nonlinear damping tended to reduce the amplitude and increase the oscillation frequency of the nonlinear vibration response. Similarly, Holubowski et al. (2019) investigated transverse vibration analysis of single wall carbon nanotube under a random load. They described the relationship between stochastic loads and the applied loads. In addition, some researchers showed their interest in single wall carbon nanotube under elastic medium. Rahmanian et al. (2016) and Fernandes et al. (2017) investigated single walled carbon nanotube on elastic foundation. They considered single parameter Winkler's foundation. They described the effects of mechanical properties and foundation stiffness on natural frequency of nanotube. Similarly, Rosa & Lippiello (2016) analysed the vibration of single wall carbon nanotube surrounded by two parameters elastic foundation. Their results showed that the influence of the nonlocal effect could be ignored in the case of specific boundary conditions. It is clear from the above discussion that the nanotube partially embedded into elastic medium under thermal load is rare in available literature.

In this paper, single wall carbon nanotube is modelled by Euler-Bernoulli beam theory and nonlocal theory of elasticity. The nanotube is partially embedded into the soil where soil is simulated by two parameters Pasternak theory. The effects of temperature on the dynamic behaviour of nanotube are analysed in different support systems. An analytical solution technique is used to solve this problem. The results obtained from this analysis are compared with the results in available literature. The results show that the natural frequency is significantly affected by the position of embedded soil and the temperature variation.

PROBLEM SETTINGS

A schematic shape of a single wall carbon nanotube is included in Fig. 1. The origin of the coordinate system is considered at the left corner point of the tube. The axis of the tube coincides with the x-axis and radius along the z-axis. The length of the tube is L and density of the material is ρ. Tube is partially supported by the elastic medium at a distance a where $0 < a < L$. Here, K_p and K_w represent spring constants for shear and compression respectively. Thermal load N is applied laterally. The main concern is to scrutinize the dynamic behaviour of nanotube.

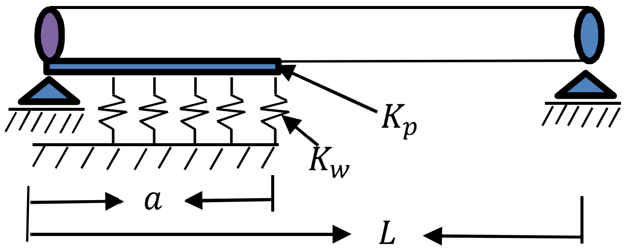

Figure 1. Nanotube partially embedded into elastic soil.

MATHEMATICAL FORMULATION

Eringen (2002) proposed the theory of nonlocal elasticity which is very effective for nanomaterial. According to his theory, the constitutive relation of nonlocal elasticity can be presented in the partial differential form as follow:

$$[1-(e_0a)^2\,\nabla^2]\sigma_{ij} = \mathrm{E}\varepsilon_{ij} \tag{1}$$

where σ, ε, e_0, a are the stress field, strain, material constant, internal characteristic length respectively. e_0a is the scale coefficient which is also called nonlocal parameter. In one-dimensional stress state, the nonlocal continuum theory with Hook's law can be presented as:

$$\sigma_{xx} - (e_0a)^2\frac{\partial^2\sigma_{xx}}{\partial x^2} = \mathrm{E}\varepsilon_{xx} \tag{2}$$

where E is Young's modulus. The displacement field can be described as:

$$u_1 = U(x,t) - z\frac{\partial W}{\partial x};\ u_2 = W(x,t) \tag{3}$$

where U and W are the axial and transverse displacements respectively. According to the Euler-Bernoulli equations, dynamic behaviour of nanotube on elastic medium can be expressed as:

$$-m_0\frac{\partial^2 W}{\partial t^2} + m_2\frac{\partial^2 W}{\partial x^2\partial t^2} + \frac{\partial^2 M}{\partial x^2} - K_wW + K_p\frac{\partial^2 W}{\partial x^2} - N\frac{\partial^2 W}{\partial x^2} = 0 \tag{4}$$

where m_0, m_2 are mass moments of inertia, K_w, K_p are spring constants for compression and shear respectively. In terms of bending moment M, the nonlocal equation can be written as:

$$M - (e_0a)^2\frac{\partial^2 M}{\partial x^2} = EI\left(-\frac{\partial^2 W}{\partial x^2}\right) \tag{5}$$

Combining Eq. (4) and Eq. (5) can be presented as:

$$\begin{aligned} EI\frac{\partial^4 W}{\partial x^4} - (e_0a)^2\frac{\partial^2}{\partial x^2}\left(K_wW - K_p\frac{\partial^2 W}{\partial x^2} + N\frac{\partial^2 W}{\partial x^2} + m_0\frac{\partial^2 W}{\partial t^2} - m_2\frac{\partial^4 W}{\partial x^2\partial t^2}\right) + K_wW \\ - K_p\frac{\partial^2 W}{\partial x^2} + N\frac{\partial^2 W}{\partial x^2} + m_0\frac{\partial^2 W}{\partial t^2} - m_2\frac{\partial^4 W}{\partial x^2\partial t^2} = 0 \end{aligned} \tag{6}$$

Deflection can be presented as the following function:

$$W(x,t) = \bar{W}(x)e^{i\omega_c t} \tag{7}$$

Using this transformation (7), partial differential Eq. (6) can be transformed in the ordinary form:

$$\begin{aligned} EI\frac{d^4\bar{W}}{dx^4} - (e_0a)^2\left(K_w\frac{d^2\bar{W}}{dx^2} - K_p\frac{d^4\bar{W}}{dx^4} + N\frac{d^4\bar{W}}{dx^4} - \rho A\omega_c^2\frac{d^2\bar{W}}{dx^2} + \rho I\omega_c^2\frac{d^4\bar{W}}{dx^4}\right) \\ + K_w\bar{W} - K_p\frac{d^2\bar{W}}{dx^2} + N\frac{d^2\bar{W}}{dx^2} - \rho A\omega_c^2\bar{W} + \rho I\omega_c^2\frac{d^2\bar{W}}{dx^2} = 0 \end{aligned} \tag{8}$$

Introducing some dimensionless parameters as follows:

$$\begin{aligned} \xi = \frac{x}{L}, w = \frac{\bar{W}}{L}, \mu = \frac{e_0a}{L},\ k_w = \frac{K_wL^4}{EI}, k_p = \frac{K_pL^2}{EI}, \omega^2 = \omega_c^2L^4\frac{\rho A}{EI} = \bar{\omega}^4, r^2 = \frac{I}{AL^2} \\ = \frac{1}{\lambda^2}, n = -\frac{NL^2}{EI} = \frac{\alpha_t\theta}{r^2} \end{aligned} \tag{9}$$

Applying the dimensionless parameters, Eq. (8) can be written as:

$$\alpha_0\frac{d^4w}{d\xi^4} + \beta_0\frac{d^2w}{d\xi^2} - \gamma_0 w = 0 \tag{10}$$

where $\alpha_0, \beta_0, \gamma_0$ can be expressed as follows:

$$\begin{aligned} \alpha_0 = \left(1 + \mu^2k_p - \mu^2n - \mu^2r^2\omega^2\right), \beta_0 = \left(\mu^2\omega^2 - \mu^2k_w - k_p + n + r^2\omega^2\right), \gamma_0 \\ = (\omega^2 - k_w) \end{aligned} \tag{11}$$

Similarly, the equation of nanotube which is out of soil or elastic medium can be presented as:

$$\alpha_1\frac{d^4w}{d\xi^4} + \beta_1\frac{d^2w}{d\xi^2} - \gamma_1 w = 0 \tag{12}$$

where $\alpha_1, \beta_1, \gamma_1$ can be expressed as follows:

$$\alpha_1 = (1 - \mu^2n - \mu^2r^2\omega^2), \beta_1 = (\mu^2\omega^2 + n + r^2\omega^2), \gamma_1 = \omega^2 \tag{13}$$

Eqs (10) and (12) are the set of governing equations for embedded nanotube and exposed nanotube respectively.

SOLUTION TECHNIQUE

In this section, an analytical technique is described for solving this problem. Elastic foundation is placed from left corner to distance a. So, the tube is divided into two segments at a distance a and two ordinary differential Eqs (10), (12) represent the behaviour of these two segments. To determine the characteristic equations, one can consider this function $w(\xi) = e^{i\delta\xi}$ as a transformation. Let consider the solution of Eq. (10) for the first segment $(0 < x < a)$ as follow:

$$w = A_1sin(\varphi_0\xi) + A_2cos(\varphi_0\xi) + A_3sinh(\psi_0\xi) + A_4cosh(\psi_0\xi) \tag{14}$$

where

$$\varphi_0 = \pm\sqrt{\frac{\sqrt{{\beta_0}^2 + 4\alpha_0\gamma_0} + \beta_0}{2\alpha_0}} \tag{15}$$

$$\psi_0 = \pm i\sqrt{\frac{\sqrt{{\beta_0}^2 + 4\alpha_0\gamma_0} - \beta_0}{2\alpha_0}} \tag{16}$$

Similarly, the solution of the Eq. (12) for the second segment $(a < x < L)$ as follow:

$$w = A_5 sin(\varphi_1\xi) + A_6 cos(\varphi_1\xi) + A_7 sinh(\psi_1\xi) + A_8 cosh(\psi_1\xi) \tag{17}$$

where

$$\varphi_1 = \pm\sqrt{\frac{\sqrt{{\beta_1}^2 + 4\alpha_1\gamma_1} + \beta_1}{2\alpha_1}} \tag{18}$$

$$\psi_1 = \pm i\sqrt{\frac{\sqrt{{\beta_1}^2 + 4\alpha_1\gamma_1} - \beta_1}{2\alpha_1}} \tag{19}$$

The Eqs (14) and (17) can be solved using the boundary conditions and intermediate conditions at the position of elastic medium.

Boundary conditions

In this paper, three different types of boundary condition are used as below:

SS: $w(0) = 0,\ w''(0) = 0, w(1) = 0,\ w''(1) = 0$

CC: $w(0) = 0, w'(0) = 0, w(1) = 0, w'(1) = 0$

CS: $w(0) = 0, w'(0) = 0, w(1) = 0, w''(1) = 0$

Intermediate conditions

Intermediate conditions are occurred due to the two different segments of the tube, those are as follows:

$$w_-(a) = w_+(a), w_-'(a) = w_+'(a)$$
$$w_-''(a) = w_+''(a), w_-'''(a) + \mu^2\omega^2 w_-'(a) = w_+'''(a) + \mu^2\omega^2 w_+'(a)$$

Using one set of boundary conditions for example simply supported boundary conditions and intermediate conditions, Eqs (14) and (17) can be expressed as follow:

$$\begin{bmatrix} -sin(\varphi_0)\varphi_0^2 & \cdots & 0 \\ \vdots & \ddots & \vdots \\ 0 & \cdots & 1 \end{bmatrix} \begin{bmatrix} A_1 \\ \vdots \\ A_8 \end{bmatrix} = 0 \tag{20}$$

The determinant of the coefficient matrix gives the value of natural frequency of nanotube.

RESULTS AND DISCUSSION

Thermo mechanical vibration of single wall carbon nanotube partially embedded into soil is investigated using exact solution technique. This vibration is influenced by some physical parameters such as nonlocal parameter, temperature as well as some geometrical parameters such as embedded length, slenderness ratio. In this section, the obtained results of the presented technique are demonstrated using various tables and graphs.

First of all, obtained results are compared with the results in available literature to examine the effectiveness of current method. Secondly, tabular data is presented to comprehend the effect of embedded length on the dynamic behaviour of nanotube. Finally, the graphs illustrate the effect of spring constant, slenderness ratio and temperature on the natural frequency of nanotube.

Table 1. Comparison of results with the results in available literature

Slenderness ratio (λ)	CC (ϖ)							
	$\mu = 0.0$		$\mu = 0.1$		$\mu = 0.2$		$\mu = 0.3$	
	(Rosa & Lippiello, 2016)	Present	(Rosa & Lippiello, 2016)	Present	(Rosa & Lippiello, 2016)	Present	(Rosa & Lippiello, 2016)	Present
10	4.5945	4.5943	4.432	4.432	4.0714	4.0715	3.6901	3.69
	7.1402	7.1401	6.3699	6.3698	5.2897	5.2898	4.5202	4.5201
	9.256	9.258	7.5757	7.5769	5.9408	5.9419	4.9776	4.9787
30	4.714	4.7139	4.5749	4.5751	4.2512	4.2513	3.8894	3.8895
	7.7557	7.7558	7.0299	7.0298	5.924	5.9242	5.0938	5.0939
	10.7106	10.7125	8.9642	8.9665	7.1222	7.1242	6.0004	6.0024
	SC (ϖ)							
	(Rosa & Lippiello, 2016)	Present	(Rosa & Lippiello, 2016)	Present	(Rosa & Lippiello, 2016)	Present	(Rosa & Lippiello, 2016)	Present
10	3.8209	3.8208	3.7099	3.7101	3.4516	3.4515	3.1621	3.1621
	6.4648	6.4647	5.8666	5.8665	4.9562	4.9563	4.2706	4.2705
	8.6516	8.6519	7.2367	7.2368	5.74	5.7396	4.8245	4.8245
30	3.9141	3.9142	3.8078	3.8078	3.556	3.556	3.2683	3.2681
	6.9867	6.9869	6.3822	6.382	5.4303	5.4305	4.6963	4.6964
	9.9591	9.9597	8.4175	8.4176	6.7218	6.7213	5.6657	5.6653

Table 1 describes the square root of frequency (ϖ) for different values of nonlocal parameter and slenderness ratio. Two different types of boundary conditions are considered such as fully clamped and clamped simply. The compressive spring constant and shear spring constant are not considered for this table. It is clear from this table that frequency decreases with increase in the value of the nonlocal parameter. Basically, increase of nonlocal parameter decreases the stress carrying capacity of the element according to the theory of nonlocal elasticity. That is why nonlocal parameter decreases the natural frequency of nanotube. On the other hand, frequency increases with increase in the value of slenderness ratio. Physically, increase the value of slenderness ratio increases length of the element. That is why, slenderness ratio increases the natural frequency of nanotube. Obtained results are compared with the paper (Rosa & Lippiello, 2016) in available literature. The results show good agreement with the results of that paper.

Table 2. Frequency of simply supported nanotube partially embedded into soil

SS		Nonlocal parameter ($\mu = 0$)			Nonlocal parameter ($\mu = 0.2$)		
Spring constant	Embedded length	$(\omega)_1$	$(\omega)_2$	$(\omega)_3$	$(\omega)_1$	$(\omega)_2$	$(\omega)_3$
$k_p = 0,$	$a = 0$	9.4155	33.4277	64.6445	7.9726	20.8141	30.2949
$k_w = 50$	$a = 0.5$	10.5419	33.6972	64.7461	9.2456	21.2559	30.5098
	$a = 1$	11.5831	33.9589	64.8476	10.4443	21.6582	30.7285
$k_p = 50,$	$a = 0$	9.4155	33.4277	64.6445	7.9731	20.8144	30.2949
$k_w = 0$	$a = 0.5$	15.3349	42.8321	72.4336	11.7803	29.2324	38.4902
	$a = 1$	23.1895	50.3242	80.8047	22.6426	42.9961	57.1836
$k_p = 50,$	$a = 0$	9.4155	33.4277	64.6445	7.9731	20.8144	30.2949
$k_w = 50$	$a = 0.5$	15.7509	43.1133	72.5195	12.0225	29.3809	38.6231
	$a = 1$	24.1504	50.6836	80.9766	23.6269	43.4102	57.4102

Table 3. Frequency of fully clamped supported nanotube partially embedded into soil.

CC		Nonlocal parameter ($\mu = 0$)			Nonlocal parameter ($\mu = 0.2$)		
Spring constant	Embedded length	$(\omega)_1$	$(\omega)_2$	$(\omega)_3$	$(\omega)_1$	$(\omega)_2$	$(\omega)_3$
$k_p = 0,$	$a = 0$	21.1074	50.9805	85.7109	16.5771	27.9824	35.3066
$k_w = 50$	$a = 0.5$	21.6269	51.1523	85.7891	17.1728	28.2481	35.4551
	$a = 1$	22.1387	51.3154	85.8672	17.7725	28.5059	35.5996
$k_p = 50,$	$a = 0$	21.1074	50.9804	85.7109	16.5771	27.9824	35.3066
$k_w = 0$	$a = 0.5$	25.8339	58.1992	92.1641	20.4512	34.6231	42.4961
	$a = 1$	31.3769	64.6523	99.1641	34.1465	53.2148	64.4258
$k_p = 50,$	$a = 0$	21.1074	50.9805	85.7109	16.5771	27.9824	35.3066
$k_w = 50$	$a = 0.5$	26.1465	58.3789	92.2266	20.5645	34.6738	42.5195
	$a = 1$	32.0801	64.9179	99.2891	34.7441	53.4961	64.5820

Tables 2, 3, 4 illustrate the three different modes of natural frequency for different values of nonlocal parameter, spring constants and different embedded lengths of nanotube. Each table is considered for specific type of boundary condition. The results describe that the frequency increases with the increase of spring constant value.

Table 4. Frequency of simply clamped supported nanotube partially embedded into soil

SC		Nonlocal parameter ($\mu = 0$)			Nonlocal parameter ($\mu = 0.2$)		
Spring constant	Embedded length	$(\omega)_1$	$(\omega)_2$	$(\omega)_3$	$(\omega)_1$	$(\omega)_2$	$(\omega)_3$
$k_p = 0,$	$a = 0$	14.5986	41.7929	74.8555	11.9131	24.5645	32.9434
$k_w = 50$	$a = 0.5$	15.5791	41.9726	74.9414	13.1455	24.8574	33.1387
	$a = 1$	16.0615	42.2148	75.0273	13.6240	25.2246	33.3027
$k_p = 50,$	$a = 0$	14.5986	41.7929	74.8555	11.9131	24.5644	32.9434
$k_w = 0$	$a = 0.5$	23.0254	50.2852	83.3516	18.6709	32.9863	41.3398
	$a = 1$	26.7949	56.9883	89.5703	27.7676	48.2227	60.9883
$k_p = 50,$	$a = 0$	14.5986	41.7929	74.8555	11.9131	24.5645	32.9434
$k_w = 50$	$a = 0.5$	23.4746	50.4961	83.4141	18.9072	33.1309	41.4961
	$a = 1$	27.6230	57.2929	89.7266	28.5449	48.5664	61.1836

Spring provides extra support as a foundation for nanotube. Increase the value of spring constant increases overall stiffness of the system. Similarly, the frequency increases with the increase of embedded length of the nanotube. Basically, an increase in embedded length increases the surface area covered by elastic medium or soil that increases the stiffness of the nanotube.

Figs 2, 3 illustrate the relationship between frequency ratio and spring constants for different values of nonlocal parameter. Two different types of end support such as fully clamped and simply supported are considered. It is clear that the frequency ratio increases with the increase of spring constant. The shear spring is more effective than the compressive spring to increase the value of frequency ratio. The frequency ratio increases rapidly at the high value of nonlocal parameter. Another way, the effect of spring constant is very significant at the high value of nonlocal parameter. The shear spring layer resists the bending moment. On the other hand, the compressive spring layer resists the deflection of the nanotube.

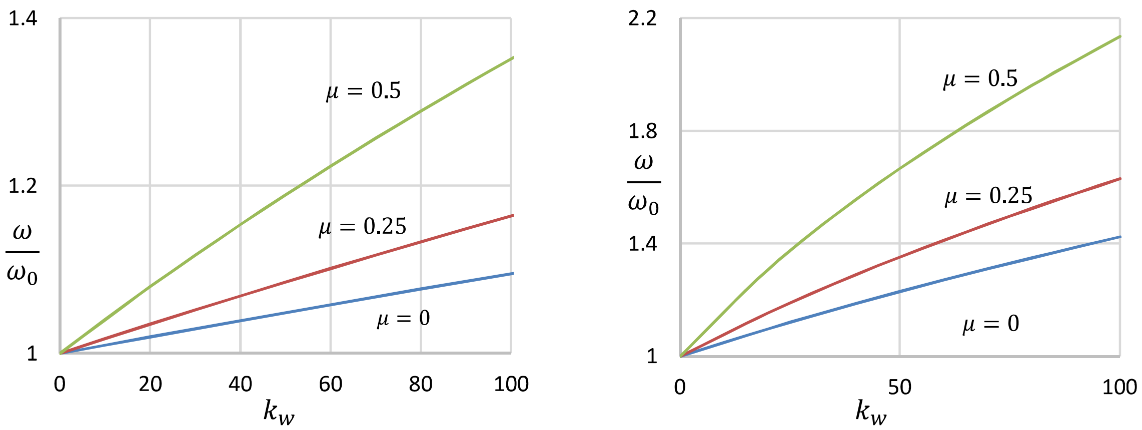

Figure 2. Frequency ratio versus compressive spring constant (k_w) for different values of nonlocal parameter (μ) in fully clamped and simply supported nanotubes.

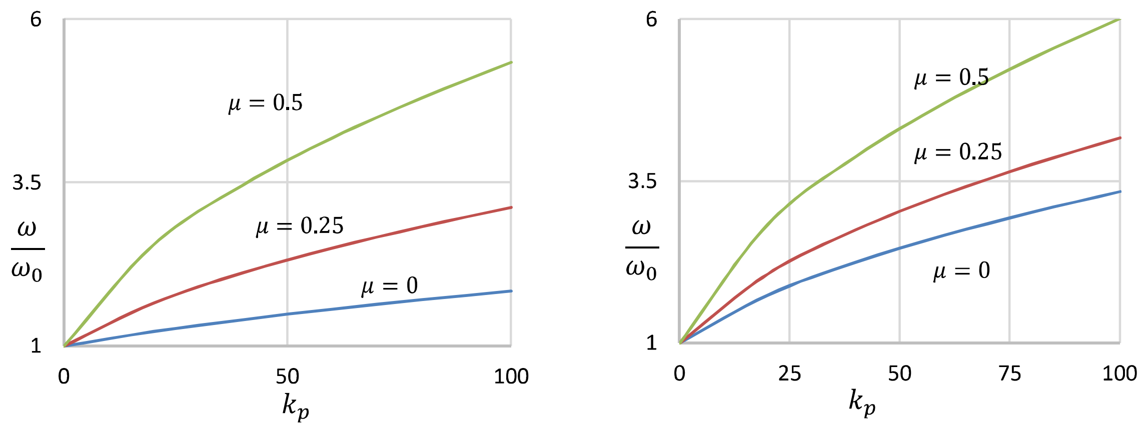

Figure 3. Frequency ratio versus shear spring constant (k_p) for different values of nonlocal parameter (μ) in fully clamped and simply supported nanotubes.

Fig. 4 demonstrates frequency for different values of slenderness ratio and temperature. Thermal expansion coefficient $\alpha_t = 1.9 \times 10^{-5}\,K^{-1}$ and nonlocal parameter $\mu = 0.1$ are considered. Frequency increases with the increase of slenderness ratio.

However, at the high temperature, frequency decreases with the increase of slenderness ratio. An increase in slenderness ratio increases the length of the nanotube that increases the frequency. On the other hand, effect of temperature increases with the increase of the length of the nanotube.

An increase in temperature reduces the strength and stiffness of the nanotube that decreases natural frequency. That is why, temperature decreases frequency in spite of high slenderness ratio.

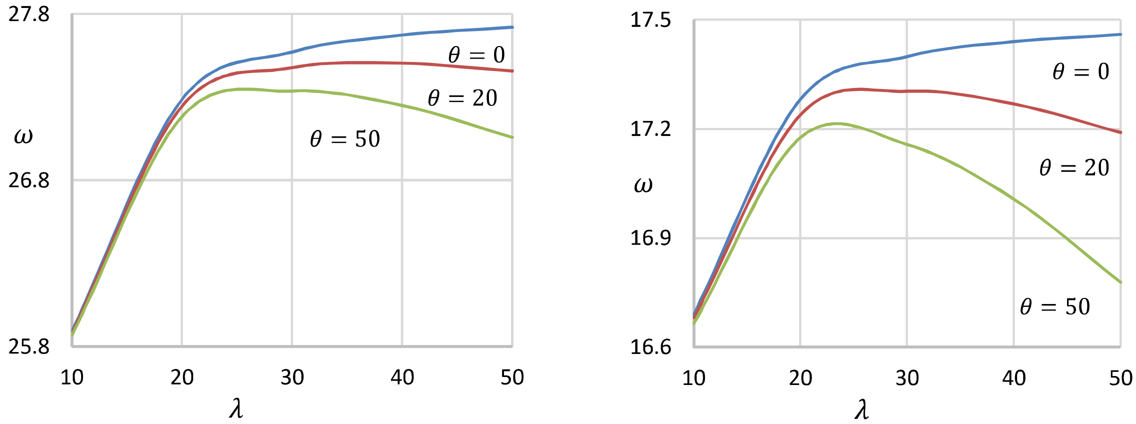

Figure 4. Frequency versus slenderness ratio (λ) for different temperatures (θ) in fully clamped, simply supported nanotubes.

Fig. 5 describes frequency ratio for different values of temperature and slenderness ratios. Simply supported and clamped supported nanotubes are considered. Thermal expansion coefficient $\alpha_t = 1.9 \times 10^{-5}\, K^{-1}$ and nonlocal parameter $\mu = 0.1$ are used. Frequency ratio increases for the increase of temperature. At the high value of slenderness ratio, frequency ratio decreases more rapidly for the change of temperature. An increase in slenderness ratio, increases length of the nanotube that increases the thermal effect. That is why at high value of slenderness ratio, frequency decreases very rapidly for the change of temperature.

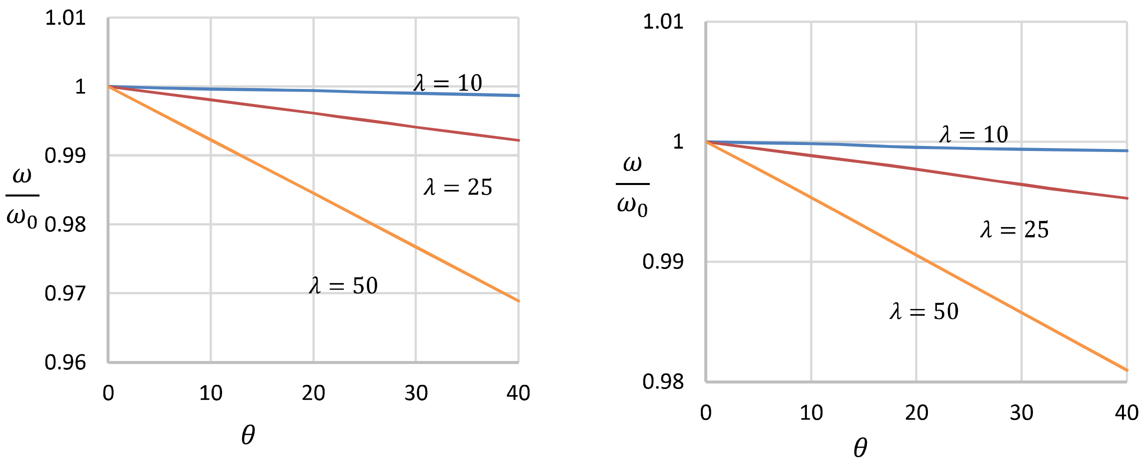

Figure 5. Frequency ratio versus temperature (θ) for different slenderness ratios (λ) in simply supported, fully clamped nanotubes.

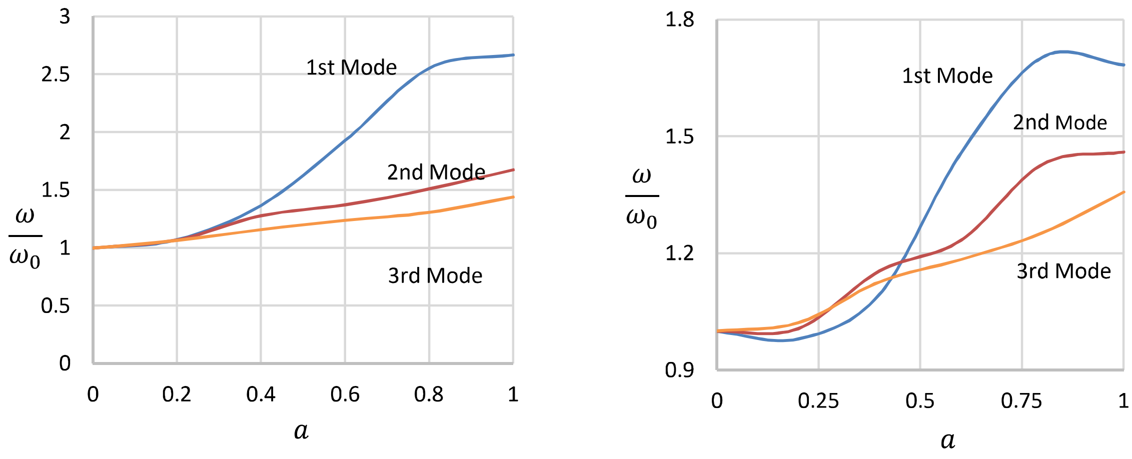

Figure 6. Frequency ratio versus embedded length (a) for different modes of frequency in simply supported, fully clamped nanotubes.

Fig. 6 illustrates the frequency ratio versus embedded length for different modes of frequency. Simply supported and clamped supported nanotubes are considered. Spring constants $k_w = 50, k_p = 50$ and nonlocal parameter $\mu = 0.1$ are used. Frequency increases with the increase of embedded length. First mode of frequency is more influenced by the embedded length than the other modes of frequency. An increase in embedded length increases the stiffness of the nanotube where the embedded length is covered by the soil which is simulated by two types of spring.

CONCLUSIONS

In the present work, analytical solution technique is introduced to analyse the dynamic behaviour of nanotube partially embedded into soil with thermal load. Soil is simulated by the two spring constants such as compressive spring and shear spring. It is clear from this analysis that the effects of nonlocal parameter, embedded length of nanotube, spring constants and temperature on dynamic behaviour of embedded nanotube are significant. At low temperature, frequency increases with the increase of slenderness ratio. On the other hand, at high temperature, frequency decreases at high value of slenderness ratio. The results of this analysis show good agreement with the results of other researchers.

REFERENCES

Aria, A.I., Friswell, M.I. & Rabczuk, T. 2019. Thermal vibration analysis of cracked nanobeams embedded in an elastic matrix using finite element analysis. *Composite Structures* **212**, 118–128.

Askari, H. & Esmailzadeh, E. 2017. Forced vibration of fluid conveying carbon nanotubes considering thermal effect and nonlinear foundations, *Composites Part B* **113**, 31–43.

Chang, T.P. 2017. Nonlinear vibration of single-walled carbon nanotubes with nonlinear damping and random material properties under magnetic field, *Composites Part B* **114**, 69–79.

Elhuni, H. & Basu, D. 2019. Dynamic soil structure interaction model for beams on viscoelastic foundations subjected to oscillatory and moving loads. *Computers and Geotechnics* **115**, 103157.

Eringen, A.C. 2002. Nonlocal Continuum Field Theories, Springer-Verlag New York, Inc., pp. 82–86.

Falope, F.O., Lanzoni, L. & Radi, E. 2020. Buckling of a Timoshenko beam bonded to an elastic half-plane: Effects of sharp and smooth beam edges. *International Journal of Solids and Structures* **185–186**, 222–239.

Fernandes, R., Borgi, S.E., Mousavi, S.M., Reddy, J.N. & Mechmoum, A. 2017. Nonlinear size-dependent longitudinal vibration of carbon nanotubes embedded in an elastic medium. *Physica E* **88**, 18–25.

Haldar, S. & Basu, D. 2013. Response of Euler–Bernoulli beam on spatially random elastic soil. *Computers and Geotechnics* **50**, 110–128.

Holubowski, R., Glabisz, W. & Jarczewska, K. 2019. Transverse vibration analysis of a single-walled carbon nanotube under a random load action. *Physica E: Low-dimensional Systems and Nanostructures* **109**, 242–247.

Jiang, J. & Wang, L. 2017. Analytical solutions for thermal vibration of nanobeams with elastic boundary conditions. *Acta mechanica solida sinica* **30**, 474–483.

Jiang, J., Wang, L. & Zhang, Y. 2017. Vibration of single-walled carbon nanotubes with elastic boundary conditions. *International Journal of Mechanical Sciences* **122**, 156–166.

Lai, S.K. & Zhang, L.H. 2018. Thermal effect on vibration and buckling analysis of thin isotropic/orthotropic rectangular plates with crack defects. *Engineering Structures* **177**, 444–458.

Malikan, M., Nguyen, V.B. & Tornabene, F. 2018. Damped forced vibration analysis of single-walled carbon nanotubes resting on viscoelastic foundation in thermal environment using nonlocal strain gradient theory *Engineering Science and Technology, an International Journal* **21**, 778–786.

Rahmanian, M., Asadi, M.A.T., Abadi, R.D.F. & Kouchakzadeh, M.A. 2016. Free vibrations analysis of carbon nanotubes resting on Winkler foundations based on nonlocal models. *Physica B* **484**, 83–94.

Rosa, M.A.D. & Lippiello, M. 2016. Nonlocal frequency analysis of embedded single-walled carbon nanotube using the Differential Quadrature Method. *Composites Part B* **84**, 41–51.

Zhang, Z., Huang, M., Xu, C., Jiang, Y. & Wang, W. 2018. Simplified solution for tunnel-soil-pile interaction in Pasternak's foundation model. *Tunnelling and Underground Space Technology* **78**, 146–158.

Zhao, L.S., Zhou, W.H., Fatahi, B., Li, X.B. & Yuen, K.V. 2016. A dual beam model for geosynthetic-reinforced granular fill on an elastic foundation. *Applied Mathematical Modelling* **40**, 9254–9268.